# Atmospheric aerosol characteristics retrieved using ground based solar extinction studies at Mohal in the Kullu valley of northwestern Himalayan region, India

Nand L Sharma[1,*], Jagdish C Kuniyal[2], Mahavir Singh[3], Pitamber P Dhyani[4], Raj P Guleria[2], Harinder K Thakur[2] and Pan S Rawat[5]

[1]*Department of Physics, Government Post Graduate College, Kullu 175 101, India.*
[2]*G.B. Pant Institute of Himalayan Environment & Development, Himachal Unit, Mohal-Kullu 175 126, India.*
[3]*Department of Physics, Himachal Pradesh University, Shimla 171 005, India.*
[4]*G.B. Pant Institute of Himalayan Environment & Development, Kosi-Katarmal, Almora 243 643, India.*
[5]*Department of Physics, Kumaun University, DSB Campus, Nainital 263 002, India.*
[*]*Corresponding author. e-mail: nlsharmakullu@hotmail.com*

Aerosol parameters are measured using a ground-based Multi-wavelength Radiometer (MWR) at Mohal (31.90°N, 77.11°E, 1154 m amsl) in the Kullu valley during clear sky days of a seasonal year. The study shows that the values of spectral aerosol optical depths (AODs) at 500 nm and the Ångstrom turbidity coefficient '$\beta$' (a measure of columnar loading in atmosphere) are high ($0.41 \pm 0.03$, $0.27 \pm 0.01$) in summer, moderate ($0.30 \pm 0.03$, $0.15 \pm 0.03$) in monsoon, low ($0.19 \pm 0.02$, $0.08 \pm 0.01$) in winter and lowest ($0.18 \pm 0.01$, $0.07 \pm 0.01$) in autumn, respectively. The Ångstrom wavelength exponent '$\alpha$' (indicator of the fraction of accumulation-mode particles to coarse-mode particles) has an opposite trend having lowest value ($0.64 \pm 0.06$) in summer, low ($0.99 \pm 0.10$) in monsoon, moderate ($1.20 \pm 0.15$) in winter and highest value ($1.52 \pm 0.03$) in autumn. The annual mean value of AOD at 500 nm, '$\alpha$' and '$\beta$' are $0.24 \pm 0.01$, $1.06 \pm 0.09$ and $0.14 \pm 0.01$, respectively. The fractional asymmetry factor is more negative in summer due to enhanced tourists' arrival and also in autumn months due to the month-long International Kullu Dussehra fair. The AOD values given by MWR and satellite-based moderate resolution imaging spectro-radiometer have good correlation of 0.76, 0.92 and 0.97 on diurnal, monthly and seasonal basis, respectively. The AODs at 500 nm as well as '$\beta$' are found to be highly correlated, while '$\alpha$' is found to be strongly anti-correlated with temperature and wind speed suggesting high AODs and turbidity but low concentration of fine particles during hot and windy days. With wind direction, the AOD and '$\beta$' are found to be strongly anti-correlated, while '$\alpha$' is strongly correlated.

## 1. Introduction

Aerosol studies especially those dealing with the estimation of their impact on climate (Seinfeld and Pandis 1998; Ramanathan *et al* 2001; Satheesh *et al* 2004) and health-related issues (Kunzli *et al* 2000) have drawn considerable attention worldwide. The role of atmospheric aerosols in modifying the regional and global radiation budget perturbing climatic balance (Russell *et al* 1994; Tegen *et al* 1996) leading to widespread ecological destruction and jeopardizing the human health is being

**Keywords.** Aerosol optical depth; Ångstrom coefficients; Multi-wavelength Radiometer; fractional asymmetry factor; meteorological parameters.

recognized by scientific community, the worldover (Penndorf 1957; McCartney 1976). Aerosols produce a variety of atmospheric effects such as formation of fog, mist and brown clouds; thereby reducing visibility in the troposphere (Kaufman and Fraser 1997; Moorthy and Pillai 2004). They influence the Earth's radiation budget and hence lead to climate forcing (Charlson *et al* 1992; Satheesh *et al* 2006) through scattering and absorption depending on their size (Ramanathan *et al* 2003), refractive index and total aerosol loading. The study of aerosols is therefore important for a number of reasons. It provides a feedback to global warming because some aerosols absorb the solar radiation resulting in warming of the atmosphere and some scatter and reflect it, resulting in cooling of the atmosphere. The net warming or cooling of the atmosphere and Earth's surface depends therefore on relative strength of absorbing and scattering aerosols at a particular place (Satheesh *et al* 2004). So, these processes of warming and cooling due to aerosols have an important role to play in the Earth's radiation budget. Its effect on human health, animal kingdom and botanical species is highly threatening (Oberdorster *et al* 1990; Dockery and Rope 1994) and dangerous.

Concerted efforts to carry out intensive research activities in India to understand and quantify the aerosols and their impact on the climate, started about a decade ago (Subbaraya *et al* 2000) when a number of Multi-wavelength Radiometer (MWR) network stations were established in different geographical locations of India as part of a project named the Aerosol Radiative Forcing over India (ARFI) taken up by the Indian Space Research Organization under the Geosphere Biosphere Programme (ISRO–GBP). However, most of these studies so far were focused in urban, semi-urban and in areas adjacent to oceans (Devara *et al* 1996; Moorthy *et al* 1997; Parameswaran *et al* 1999; Pant *et al* 2006). The study of aerosols at high altitude sites similar to any other site is helpful in understanding the atmospheric boundary layer (ABL) dynamics, visibility change and precipitation in mountainous regions. Large aerosol concentration does not allow cloud droplets to grow and thereby, results in inhibiting rain, decreasing visibility and lowering ABL; while lower concentration of aerosols leads to a growth of cloud condensation nuclei up to proper size and produces precipitations (Jayaraman 2001; Pant *et al* 2006; Dumka *et al* 2008). Further, aerosol studies in the various parts of the Himalaya have gained interest in the context of ever-increasing transport of aerosols from the Sahara and Thar Deserts to the Himalayan foothills due to their blockade by its high mountain ranges and consequently have an adverse impact on glaciers (Gautam *et al* 2009). Also, the investigations of aerosol characteristics from remote hilly areas are important in providing not only background values of aerosol parameters (against whom the urban values can be compared), but also to assess the impact of anthropogenic activities on the Himalayan ecosystem which is topographically very fragile and ecologically very delicate (Moorthy *et al* 1998, 2007, 2008). This has led to the

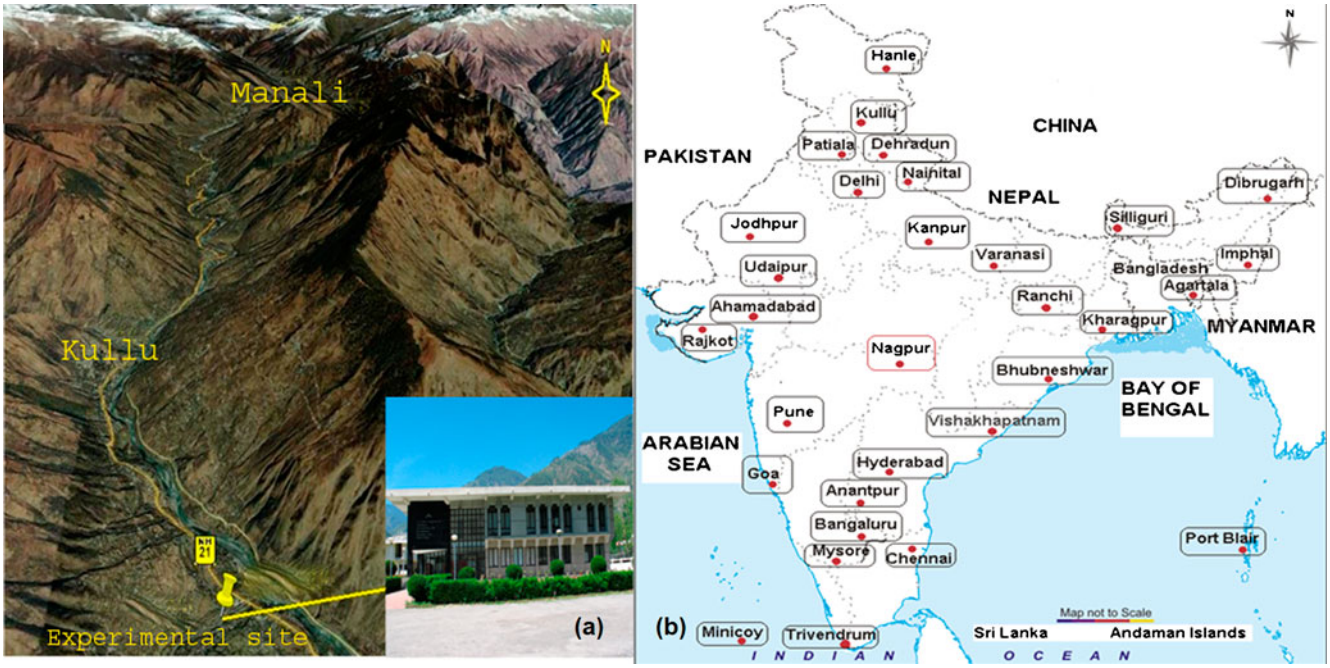


Figure 1. (**a**) Topography of experimental area and (**b**) MWR stations under ARFI project of ISRO–GBP program.

establishment of MWR stations (figure 1b) under the ISRO–GBP at Mohal-Kullu in Himachal Pradesh (Kuniyal *et al* 2006) and also at few other locations such as Nainital in Uttarakhand (Pant *et al* 2006) and Dibrugarh in Assam (Bhuyan *et al* 2005) only recently. The data at these stations are collected by MWR developed by Space Physics Laboratory, Thiruvananthapuram, which is operated regularly on clear sky days when no visible clouds are near the solar disc.

The ever increasing anthropogenic interferences due to socio-economic activities, population growth, tourism-related activities and hydropower excavation are steadily jeopardizing the existing Himalayan ecosystem which once was world famous for its clean and pristine environment (Kuniyal *et al* 2004). So, temporal variations of aerosol parameters such as spectral aerosol optical depths (AODs) and Ångstrom coefficients have to be estimated in order to investigate impacts of anthropogenic activities (Jayaraman 2001) and long range transport from polluted to clean areas of the Himalayan region so that remedial measures can be initiated accordingly to save this important ecosystem of the world.

The extinction of solar radiation by aerosols is given by a parameter called columnar AOD. It is the integration of extinction coefficients along vertical column of unit cross-section from the Earth's surface to the top of the atmosphere (Satheesh *et al* 2004). It is a first indicator to know the extent of particulate matter in the atmosphere at a particular place. The Ångstrom parameters '$\alpha$' and '$\beta$' are another set of numbers that give an idea about relative abundance of fine to coarse size particles and turbidity in atmosphere, respectively (Ångstrom 1964; Iqbal 1983; Tomasi *et al* 1983). The present study therefore aims at monitoring the air for aerosol parameters – AODs and Ångstrom coefficients and finding their correlation with meteorological parameters at Mohal (Kullu) in the northwestern Indian Himalaya. This would help in unfolding the current status of air quality in this part of the Himalaya during clear sky days from April 2006 to March 2007.

## 2. Experimental site and database

### 2.1 *Site description*

Observations were carried out at Mohal (31.90°N, 77.11°E, 1154 m amsl), 5 km south of a famous tourist spot and district headquarters – Kullu in Himachal Pradesh state of India using a MWR. The Himachal Unit of G. B. Pant Institute of Himalayan Environment & Development (GBPI-HED) is located here. This site lies in the Lesser Himalayan zone and mid in altitude when compared to the higher (the Great Himalaya) and foothill (the Siwalik) zones of the Himalaya. The experimental site topographically is a gentle slope region flanked by North–South running mountain ranges of height ranging from 3000–5000 m on either side. The Kullu valley, where the present study site exists, is located between these two inclined mountain ranges. River Beas flows through the middle of this valley. This valley begins from Larji (31.74°N, 77.23°E, 957 m amsl) in the lower Beas basin in the south and stretches up to Rohtang Crest (32.37°N, 77.25°E 4038 m amsl) in the upper Beas basin in the north (Gajananda *et al* 2005). The area is endowed with rugged mountainous topography in most of the eastern side and evergreen forests in the western side. The topographic map of the valley is shown in figure 1(a). It is also one of the ARFI network stations (figure 1b). It is a semi-rural location about 100 m away from National Highway-21. Kullu municipal town, 5 km north of the present experimental site has a native population of 18,306 inhabiting an area of about 7 km$^2$ (Kuniyal *et al* 2007). The population of the entire Kullu valley, which constitutes Kullu and Manali subdivisions of Kullu district and some part of Sadar Division of Mandi District was 221,858 (Census of India 2001). The Kullu valley is an important tourist destination of the western Himalaya. It has witnessed a tremendous growth in tourists' inflow as well as vehicular influx in the recent decades (Kuniyal *et al* 2004). It is evident from the fact that from 2004 to 2008, the total tourist traffic in the entire state of Himachal Pradesh increased from 6.55 to 9.75 million, out of which Kullu and Manali alone hosted 2.12 million tourists in 2008 (Sharma *et al* 2009). Also, according to the Regional Transport Office, Kullu, there are about 30,000 vehicles of all types including two-wheelers, registered until date in the district and every year about 1000 vehicles are registered at each of the three subdivisions of this valley. The valley which earlier was famous as 'the Valley of apples' has nowadays become a jungle of concrete, in terms of construction of large numbers of hotels, business establishments, hydropower colonies and a large number of tourism-related activities.

### 2.2 *Prevailing meteorology*

The lower part of the Kullu valley, from Aut to Katrain, is situated in the rain shadow zone where most of the rain is received during winter. Heavy snowfall takes place in the winter months in the valley as well as on adjoining hilltops around the experimental site, while once or twice in winter, it falls at the bottom of the valley but melts within

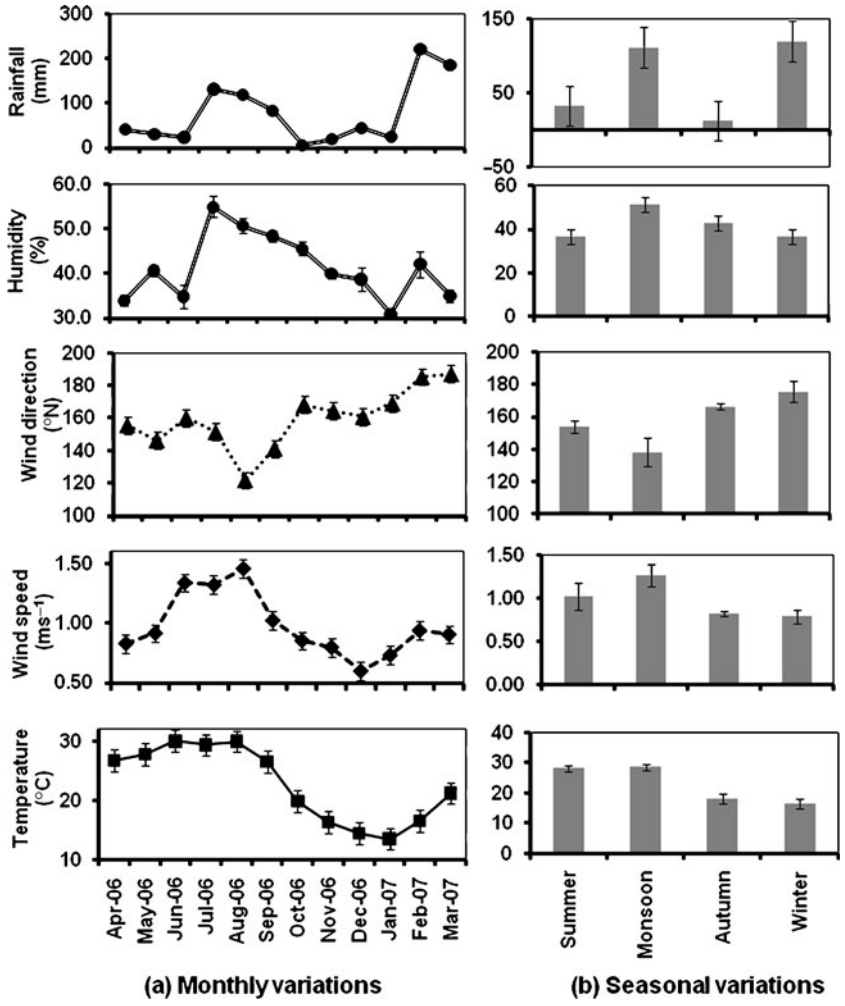


Figure 2. Meteorological conditions during MWR measurement days at the experimental site.

moments due to increasing temperature. Figure 2 shows meteorological conditions during MWR operating days of the study period on monthly and seasonal basis. On an average, it shows that the temperature slowly rises from 26.7°C in April up to 30°C in the peak summer month of June. It remains high in monsoon months although it becomes slightly less and then decreases in the last monsoon month of September, gradually becoming the lowest with 13.5°C in the winter month of January. Finally, it rises again up to 21.2°C in March. On a seasonal basis, the temperature is high during summer and monsoon and lowest in winter. Wind speed has almost a similar trend as temperature, showing increase from 0.83 m/s in April to 1.46 m/s in August, then it gradually decreases to 0.60 m/s in December and finally increases gradually up to 0.91 m/s in March. Wind speed is highest during monsoon months while it is lowest in winter. The wind blows towards the present experimental site at Mohal mostly from the southeast and/or from the Indo-Gangetic Plains (∼135°N) in summer as well as in monsoon months while a gradual change in wind direction takes place from the south of the Thar desert region to the present study site (∼180°N) in autumn and winter. In essence, wind gradually changes its direction from the south-east (or from Indo-Gangetic Plains) in summer to south-west (or from the Thar Desert in India) in winter. The relative humidity is low in summer but is the highest with 55% in July during monsoon. Thereafter, it decreases sharply in autumn and reaches its lowest value of 31% in the winter month of January. Also, the rainfall is highest at 221 mm in February and lowest at 6 mm in the autumn month of October. Seasonally, highest rainfall is 120 mm in winter and lowest is 13 mm in autumn. Based on similar prevailing meteorological conditions for longer periods suggest that the climate in this part of the region locally has four distinct seasons; summer (April to June), monsoon (July to September), autumn (October and November) and relatively longer and harsh winter (December to March). March is sometimes pleasant and is also called spring season (Kuniyal *et al* 2004).

### 2.3 *Methodology*

The ground-based MWR developed and designed by the Space Physics Laboratory (SPL), Vikaram Sarabai Space Centre, Trivandrum is used to retrieve AODs. The MWR contains 10 filters of wavelengths 380, 400, 450, 500, 600, 650,750, 850, 935 and 1025 (in nm) allowing light from ultraviolet to near-infrared region to pass through it in steps with the help of automatic filter wheel motion. The radiation passes through a field of view (FOV) limited to $\sim 2^\circ$ using lens pin-hole detector optics, so that the effect of diffuse radiation entering into the FOV on the retrieved optical depths may be insignificant (Moorthy *et al* 1998). The instrument is semi-automatic in nature. Before tracking the Sun, the optical unit is mechanically adjusted on an equatorial mount and is allowed to move at every 12 s around the orthogonal axis with an angular speed equal to the Earth (i.e., $0.05^\circ$ in 12 s) in order to keep the MWR always aligned towards the Sun. It works on the principle of measuring solar extinction using Lambert–Beer law (Shaw *et al* 1973); according to which flux of solar radiation at the Earth's surface is given by Moorthy *et al* (1999)

$$F_\lambda = F_{o\lambda} \left(r_o/r\right)^2 \exp\left(-m\tau_\lambda\right). \tag{1}$$

Here $F_\lambda$ and $F_{o\lambda}$ represent solar flux at the Earth's surface and at the top of the atmosphere respectively, while $r_o$ and $r$ denote the mean and instantaneous Sun–Earth distance, respectively. Whereas '$m$' denotes the relative airmass representing relative increase in optical path with increase in zenith angle and $\tau_\lambda$ is wavelength-dependent optical depth. MWR converts the above flux into voltage (Moorthy *et al* 1994) as follows:

$$V_\lambda = V_{o\lambda} \left(r_o/r\right)^2 e^{-m\tau_\lambda}. \tag{2}$$

Taking natural log on both sides

$$\ln V_\lambda = \ln\ V_{o\lambda} + 2\left(\ln r_o/r\right) - m\tau_\lambda. \tag{3}$$

The plot of $\ln V_\lambda$ along $y$-axis with '$m$' along $x$-axis is called the Langley plot and is a straight line during the period when $\tau_\lambda$ is constant. It helps in finding AOD ($\tau_\lambda$) as slope of best fit line. The $Y$-intercept for $m = 0$ yields $V_{o\lambda}$, which is proportional to $F_{o\lambda}$ (the flux at the top of atmosphere) and remains invariant over the years. Long-term stability of this intercept corrected for daily Sun–Earth distance is an indicator of unchanged MWR parameters and hence it is an indirect calibration of the instrument (Gogoi *et al* 2008). For every filter, this intercept should remain within 10% of its long-term values and if it is found high, then it indicates deterioration of that filter and is not used for further analysis. During the study period, the stability of the instrument was fairly good, with the Langley intercept having standard deviation of 6.8% and 7% for forenoon (FN) and afternoon (AN) values, respectively. When significant deviation was observed for a few days, these data were not considered for further analysis. The variance in $Y$ intercept for $m = 0$ at 850 nm frequently appeared more than 10% during the study period and hence appears unstable. Therefore, the data corresponding to this filter are not considered in the present analysis. The total columnar AOD ($\tau_\lambda$) is a result of scattering by air molecules, absorption by ozone, extinction by water vapours and by aerosols present in the atmosphere, i.e.,

$$\tau_\lambda = \tau_{m\lambda} + \tau_{o3\lambda} + \tau_{w\lambda} + \tau_{p\lambda}. \tag{4}$$

The AOD contributed by aerosols ($\tau_{p\lambda}$) can be deduced from $\tau_\lambda$ if $\tau_{m\lambda}$, $\tau_{o3\lambda}$ and $\tau_{w\lambda}$ are estimated separately, i.e.,

$$\tau_{p\lambda} = \tau_\lambda - \left(\tau_{m\lambda} + \tau_{o3\lambda} + \tau_{w\lambda}\right). \tag{5}$$

The contribution from gaseous molecules, ozone and water vapours is estimated analytically using reference atmospheric profiles. Errors and uncertainties in the retrievals of AOD at any wavelength (Russell *et al* 1993) are given by:

$$\begin{aligned}\delta\tau_{p\lambda} = {} & \left[\tau_{p\lambda}\left(\delta F/F\right)\right]^2 + \left[\tau_\lambda\left(\delta m/m\right)\right]^2 \\ & + \left[1/m\left(\delta V_{o\lambda}/V_{o\lambda}\right)\right]^2 + \left[1/m\left(\delta V_\lambda/V_\lambda\right)\right]^2 \\ & + \left[\Delta\tau_\lambda\right]^2.\end{aligned} \tag{6}$$

The first term on the right hand side of the above equation represents the error due to diffused scatter radiation, the second term is error due to 1-s resolution in time for airmass calculation, the third term represents the error due to uncertainty in the Langley intercept and the fourth term represents uncertainty in the MWR output. These errors if added produce a total error <0.02. The fifth term represents the total error due to atmospheric models and its value is generally <0.01. Ozone models may contribute to an uncertainty of 0.003 at wavelengths between 500 and 650 nm. The AODs may therefore have maximum uncertainty of $\sim$0.03. Additional details of the instrument, data analysis and calibration measurements used in the present study have been published elsewhere (Moorthy *et al* 1997, 1999; Gogoi *et al* 2008).

Temporal variation of AODs at all wavelengths is investigated for all clear sky days. A factor which gives amount by which FN–AODs differ from AN–AODs called fractional asymmetry factor (AF) and is calculated on monthly and annual basis using formula (Ganesh *et al* 2008) as follows:

$$\mathrm{AF} = \left(\mathrm{FN\_AOD} - \mathrm{AN\_AOD}\right)/\mathrm{FN\_AOD}. \tag{7}$$

During bad weather conditions, the ground-based MWR observations are not sufficient in assessing the regional distribution of aerosols. To obtain a more homogeneous picture of aerosol environment over this region, we attempted to compare our data with satellite-derived observations. The moderate resolution imaging spectro-radiometer (MODIS) is a key instrument present onboard the polar earth observing system (EOS) Terra and Aqua satellites sensing morning and afternoon part of each day (Levy *et al* 2007). It imparts valuable information about the global distribution of aerosols as it has a large spectral coverage of 36 wavelengths, large swath of 2330 km and accuracy within an uncertainty limit of $\Delta\tau_{p\lambda} = \pm 0.05 \pm 0.15\tau_{p\lambda}$ over the land (Remer *et al* 2005; Aloysius *et al* 2008). The reflectance observed from these 36 filters is used to find many parameters such as temperature, humidity, ozone, AOD, Ångstrom coefficients, scattering albedo, etc., on the Earth's surface, clouds as well as on the oceans. Seven wavelengths ranging from 470–2130 nm are used to retrieve AODs and hence to estimate Ångstrom coefficients, out of which AOD at 550 nm filter is, used for present AOD comparisons. To improve reflectance from desert or white surfaces such as snow covered area like ours, in the MODIS, three wavelengths as Deep Blue algorithm have been provided. The large swath area of MODIS covers almost all the places in the globe almost daily (http://modis-atmos.gsfc.nasa.gov/_docs/ATBD_MOD04_C005_rev2.pdf).

MODIS has, however, known problems in retrieving AOD over land. However, in the Indian context, validation of MODIS-derived AOD has been attempted by many researchers (Tripathi *et al* 2005; Gogoi *et al* 2008; Sharma *et al* 2010). The latest updated MODIS algorithm (version 5) shows improved correlation with worldwide AERONET sun photometers (Prasad and Singh 2007; Misra *et al* 2008). Nowadays, improved empirical relations regarding surface reflectance parameterization to get around the biggest obstacle hindering the aerosol remote sensing (Kaufman *et al* 1997; Ganguly *et al* 2006) have been developed and used in MODIS. In spite of all these advantages, ground-based observations provide benchmark to assess validity and efficacy of both MODIS as well as ground-based instruments such as MWR. The ground-based observations suffer from human errors while MODIS algorithms can be improved from ground-based observations. The MODIS-derived AODs at 550 nm (Kaufman *et al* 2003) are compared with MWR-derived AODs which are interpolated to 550 nm using the Ångstrom formula.

$$\tau_{550} = \tau_{500}\,(550/500)^{-\alpha}. \tag{8}$$

From substitution of optical depth at 500 nm ($\tau_{500}$) retrieved from MWR and value of Ångstrom wavelength exponent '$\alpha$' estimated from MWR data in equation (8), we get the calculated value of ground-based AOD at 550 nm ($\tau_{550}$).

Also, the correlation between AOD at 500 nm, '$\alpha$', '$\beta$' and corresponding mean value of meteorological parameters retrieved from Automatic Weather Station installed at our site, was estimated using student's '$t$' distribution formula (Goyal and Sharma 1963)

$$t = r\,sqrt\,(n-2)\,/sqrt\left(1-r^2\right), \tag{9}$$

where '$r$' is the correlation coefficient, $n$= number of data points, and $n-2$= degree of freedom. The '$t$' thus calculated is used to find probability Ps of correlation outside the region of significance under two-tailed column in $t$-table. The value of Ps is used to find the percentage of the level of confidence (% CL) of correlation (Ps<0.01≥ CL>99%, etc.).

The Ångstrom coefficients ('$\alpha$' and '$\beta$') are calculated using Ångstrom relation (Ångstrom 1961) as:

$$\tau_{p\lambda} = \beta\,\lambda^{-\alpha} \tag{10}$$

$$\ln\,\tau_{p\lambda} = \ln\,\beta - \alpha\,\ln\,\lambda. \tag{11}$$

The graph between log of AOD values and log of corresponding wavelength will be a straight line. Its intercept gives log $\beta$ and slope gives $-\alpha$ (Schuster *et al* 2006; Kaskaoutis *et al* 2007). While calculating '$\alpha$' and '$\beta$', we use one set of AOD values of FN and one set of AN of a particular measurement day at 10 wavelengths. Out of these, AOD value at 850 nm is not taken due to instability of this filter, while AOD value at 935 nm is not taken due to the fact that it is mostly linked to water vapours present in the atmosphere (Moorthy *et al* 1991). So we get one value of '$\alpha$' and one value of '$\beta$' for FN part and similarly one set of values for AN part of each measurement day.

## 3. Results and discussion

### 3.1 *Seasonal and annual variations of AOD*

Figure 3 shows variation of monthly mean AOD at 500 nm for all 79 clear sky days during April 2006 to March 2007. It shows that monthly FN-AOD at 500 nm is high in summer, decreases in monsoon and becomes lowest in autumn; thereafter it increases in winter. It has slightly less increase in pleasant spring month of March but has exceptionally more values in the rainy month of August, and in the two winter months of December and January. The AN-AOD at 500 nm decreases from April to December with exceptionally less decrease

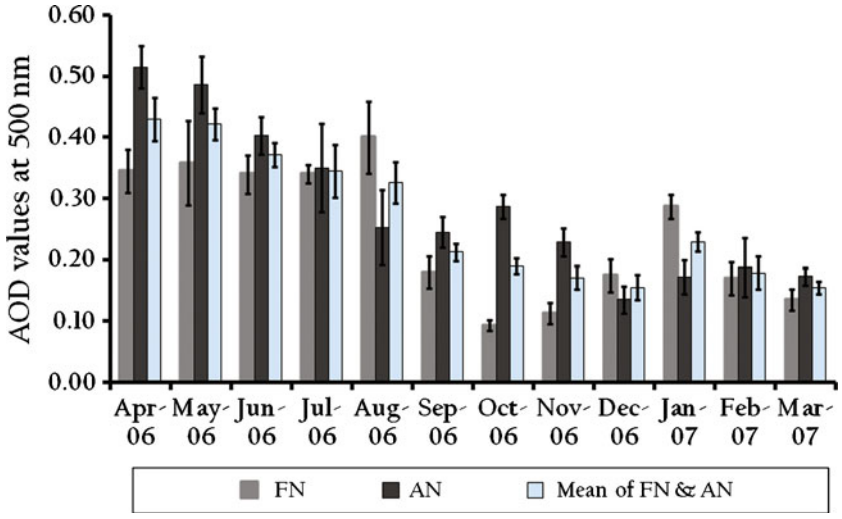


Figure 3. Variations of monthly mean AOD at 500 nm.

in October and November and rises thereafter. The mean AOD at 500 nm is high in summer, moderate in monsoon, low in winter and lowest in autumn; a trend found at many of the locations. On an average, the AOD at 500 nm is found to be $0.41 \pm 0.03$ in summer, $0.30 \pm 0.03$ in monsoon, $0.18 \pm 0.01$ in autumn and $0.19 \pm 0.02$ in winter season. These values are higher when compared to sloppy hill sites like Mauna Loa, Nainital and Hanle (Shaw 1982; Holben *et al* 2001; Dumka *et al* 2008; Verma *et al* 2010) but are less than at valley type of hill sites like Mongu, Cape Verde and Dibrugarh (Jaenicke and Schutz 1978; Eck *et al* 1999; Chiapello *et al* 1999; Gogoi *et al* 2008). Annual mean AOD at 500 nm is found to be $0.24 \pm 0.01$ for all clear sky days of study period, while during land campaign for March and April; this value of AOD at Mohal at the same wavelength with the help of Microtops II Sunphotometer shows $0.26 \pm 0.03$ (Kuniyal *et al* 2009).

### 3.2 *Fractional asymmetry factor of AOD*

The deviation of FN-AOD from AN-AOD is given by fractional asymmetry factor and is calculated using equation (7). Its negative value indicates increase in AN-AODs while positive value shows decrease in FN-AODs. The asymmetry factor at a particular wavelength for various months (monthly) and that of all wavelengths in particular month (spectral) is shown in figure 4(a and b), respectively. From figure 4(a), as expected, AF is seen negative for most of the months at all wavelengths because mornings are mostly clear and evenings become more turbid due to day-long increased human activities at a place. This negative AF is slightly more in the summer months of April and May due to increased number of tourists. However, it is significantly more in the autumn months of October and November due to month long International Kullu Dussehra fair in the valley. This is because during this fair, people start gathering everyday mostly during afternoon hours after finishing their routine work to watch entertaining programmes and for purchase of household items for the oncoming winter months. This important cultural event continues for about a month starting mostly from mid-October to mid-November. This gathering of people and plying of vehicles in large numbers causes production of huge dust which increase AN-AOD. From figure 4(b), it is also seen that the negative AF is highest at 380 nm and thereafter it decreases to its lowest level at 1025 nm, during almost all the months. It indicates that more fine particulate matter is generated from forenoon to afternoon during these months. From figure 4(a), it is also seen that during August, December and January, AF is positive at all wavelengths while in July and September, it is positive only at higher wavelengths; 935 nm and 1025 nm. These positive values in monsoon months are possibly due to frequent early morning fog in these months which attach water on hygroscopic aerosol particles, increasing particle size and hence the morning AODs (Shaw 1976; Wang *et al* 2008) and with the passing of day, this moisture on particles evaporates. In winter months, the reason for positive AF values is a reduced sunlight leading to overall low aerosol production in the evening and also more pollutants capped in shallow inversion layer in the morning which breaks with passage of day due to solar heat and pollutants possibly getting convected away by noon and thereafter (McCartney 1976). From figure 4(b), it is also observed that the positive value of AF is almost the

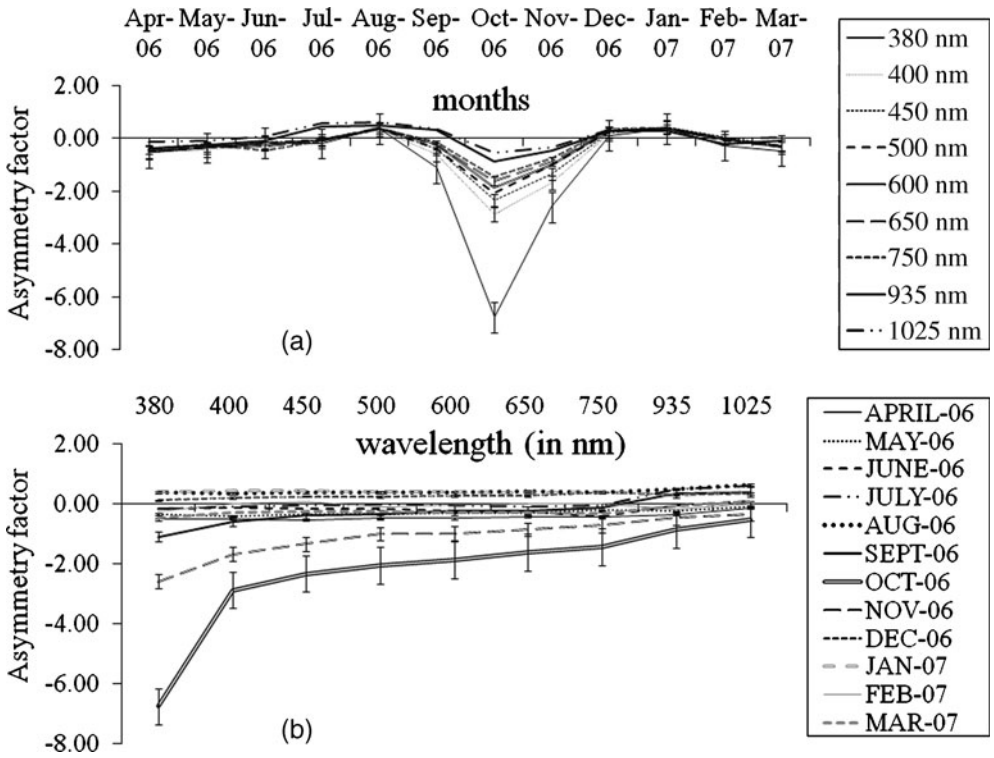


Figure 4. Fractional asymmetry factor (**a**) monthly and (**b**) spectral.

same at all wavelengths showing that during these months, contribution of fog and capped pollutant in the shallow inversion layer to increase morning AOD and rate of evaporation and transporting away of particles to decrease afternoon AOD, is equal for particles of all sizes.

### 3.3 *Spectral variations of AODs and temporal variations of Ångstrom parameters*

The spectral AOD graphs for different months are depicted in figure 5 and it shows a gradual decrease in AOD with wavelengths indicating abundance of fine particles over coarse particles in our atmosphere. The low slope at first filter during some months indicates somewhat low production of ultra-fine particles. The increase in AOD at 1025 nm during all months shows relatively more concentration of coarse particles of relatively larger sizes. These exponential variations of AODs with wavelengths for each month are consistent with the Ångstrom relation given by equation (10). The constants '$\alpha$' and '$\beta$' given in this equation are not constants throughout a year, but also have temporal variations. The monthly mean values of '$\alpha$' and '$\beta$' as calculated using equation (11) are shown in figure 6. It shows that '$\alpha$' is low in summer, increases to moderate level in monsoon and becomes high in

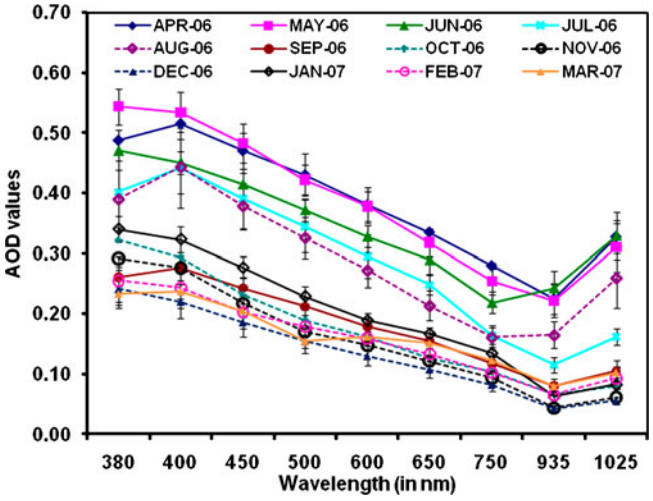


Figure 5. Spectral AOD variations during various months of study period.

autumn and early winter months, while in later winter months, it again starts decreasing. The mean value of '$\alpha$' for summer is 0.64 ± 0.06, for monsoon 0.99 ± 0.10, for autumn 1.52 ± 0.03 and for winter 1.20 ± 0.15. The converse is the case of beta for which seasonal mean values are high (0.27 ± 0.01) in summer, low (0.15 ± 0.03) in monsoon and lowest (0.07 ± 0.01) in autumn, but increases again up to 0.08 ± 0.01 in winter. Such

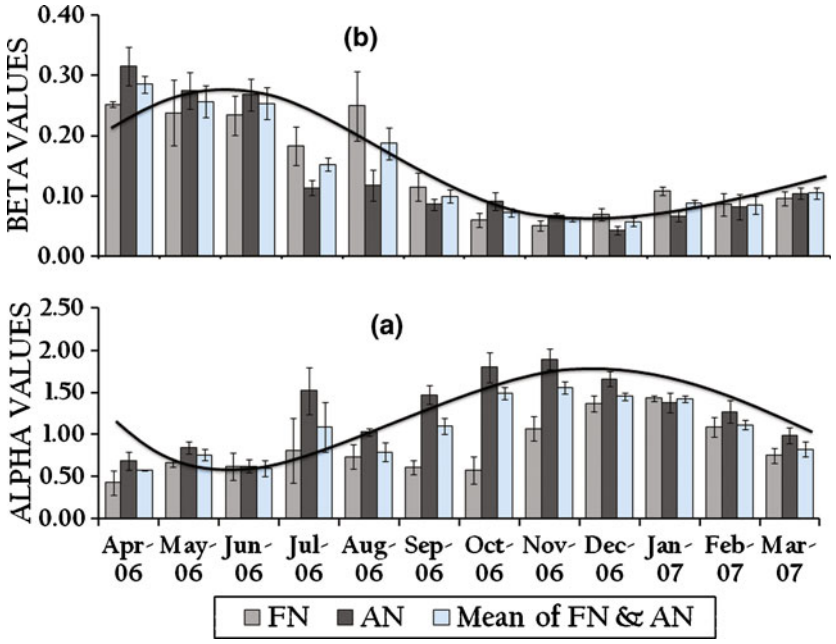


Figure 6. Monthly mean values of (**a**) wavelength exponent '$\alpha$' and (**b**) turbidity coefficient '$\beta$'.

a trend has been found at many sites in India and abroad having similar geographical locations (Devara *et al* 2005; Kumar *et al* 2007; Xin *et al* 2007). The relatively higher value of '$\alpha$' in May can be attributed to peak tourists' inflow, while in July it is considered due to continental convective drift of fine dusts brought by pre-monsoon winds. The slightly low value in August is possibly due to the washout effect and high value in autumn months is due to a month-long Kullu Dussehra festival in the valley. It may be pointed out that '$\beta$' has same monthly and seasonal variations as AOD while '$\alpha$' has an opposite trend to AOD as well as '$\beta$' consistent with equation (10). The annual mean values of '$\alpha$' and '$\beta$' are $1.06 \pm 0.09$ and $0.14 \pm 0.01$, respectively.

Further, the correlation between FN, AN and mean values of '$\alpha$' and '$\beta$' for various measurement days of a particular month (monthly correlation) as well as between monthly mean values of various months (annual correlation) was calculated which is shown in table 1. It is found mostly negative; a result consistent with most of the researchers (Devara *et al* 2005; Maheskumar *et al* 2007; Gogoi *et al* 2008). There are a few exceptions of positive correlation which is also called anomalous correlation (Ganesh *et al* 2007). It is seen that there is a negative correlation for almost all the months except November and March during FN part of the measurement days and July, August and December during AN part of the measurement days. The whole-day correlation is negative in all the months except November and December. The positive anomalous correlation found mostly during monsoon and winter months, suggests that during these months both fine and coarse particle strength is of supplementary nature, i.e., more fine particles, more turbidity and *vice-versa*. The reason for this in these months could be the convective airmass transport from or towards far-off places raising or lowering both simultaneously (Gogoi *et al* 2008). On an annual basis, this correlation is significantly negative in all the parts of a day, although it is slightly weaker in FN part of a day than in the AN part.

### 3.4 *Comparison with MODIS data*

Figure 7 shows the comparison of daily, monthly and seasonal mean AODs at 550 nm over Mohal derived from MODIS and calculated for ground-based MWR using equation (8). The scatter plot of all diurnal AODs at 550 nm values shown in figure 7(a) indicates good agreement between two sets of values with a mean absolute difference (MABD) of 0.06, root mean square difference (RMSD) of 0.08 and correlation coefficient of 0.76. It shows the slope of 0.9620 towards MODIS-derived AODs indicating a slight over-estimation of diurnal AODs by MODIS. Monthly variations depicted by figure 7(b) shows good agreement in the trend as well as in the magnitude of two sets of values with MABD of 0.03, RMSD of 0.05 and correlation coefficient of 0.92. Except some noticeable differences in the month of April, September and November of 2006 and January of 2007, MODIS and MWR AODs in all other months

Table 1. *Correlation between α and β.*

| Part of the day | | Monthly correlation | | | | | | | | | | | | Annual correlation |
|---|---|---|---|---|---|---|---|---|---|---|---|---|---|---|
| | | Apr-06 | May-06 | Jun-06 | Jul-06 | Aug-06 | Sep-06 | Oct-06 | Nov-06 | Dec-06 | Jan-07 | Feb-07 | Mar-07 | |
| FN | Count | 2 | 5 | 7 | 3 | 4 | 11 | 3 | 6 | 7 | 13 | 5 | 13 | 12 |
| | r | −1.00 | −0.99 | −0.91 | −0.99 | −0.93 | −0.45 | −0.99 | 0.06 | −0.37 | −0.14 | −0.65 | 0.54 | −0.55 |
| | %CL | −99 | −99 | −99 | −90 | −70 | −80 | −90 | 10 | −60 | −30 | −70 | 90 | −90 |
| AN | r | −1.00 | −0.64 | −0.79 | 0.99 | 0.79 | −0.08 | −0.97 | −0.25 | 0.01 | −0.13 | −0.74 | −0.37 | −0.82 |
| | %CL | −90 | −70 | −95 | 95 | 60 | −20 | −80 | −40 | 10 | −30 | −80 | −70 | −99 |
| Mean | r | −1.00 | −0.95 | −0.99 | −0.28 | −0.59 | −0.76 | −0.98 | 0.66 | 0.33 | −0.76 | −0.50 | −0.81 | −0.88 |
| | %Cl | −99 | −98 | −99 | −20 | −40 | −98 | −80 | 80 | 50 | −99 | −60 | −99 | −99 |

are in good agreement. The seasonal comparisons shown by figure 7(c) again indicate that MODIS and MWR values are almost the same except in autumn. These seasonal values have excellent agreement with MABD of 0.03, RMSD of 0.04 and correlation coefficient of 0.97. The higher difference in some months and seasons can be ascribed to an invisible cirrus cloud or an inappropriate choice of the aerosol model in the MODIS retrieval algorithm. Thus, MWR-retrieved AODs match well with MODIS-derived values with the difference lying within instrumental uncertainties and so effectively characterize AOD distribution over Mohal.

### 3.5 *Correlation between AODs and meteorological parameters*

The correlation coefficients between AODs at 500 nm and meteorological parameters calculated using equation (9), on monthly as well as on annual basis are shown in table 2. It shows that except for few winter months, there is a positive correlation of temperature with AOD in most of the months. This indicates an increase in AOD with temperature and *vice versa*. This positive correlation is strong in monsoon, moderate in autumn, and weak in summer. This is an expected trend as rising temperature favours fog to condense on aerosol particles in monsoon months, produces more dust due to wilting of dried leaves in autumn and withering of clay in summer months, thereby raising AODs. In winter, negative correlation of temperature shows that AOD decreases with increasing temperature and *vice versa* and the reason for this could be the breaking of shallow inversion layer and possible convective drift of pollutants away from this region. Table 2 also shows that this correlation is significantly positive with mean correlation coefficient of 0.77 and level of confidence above 99% on an annual basis. Further, this correlation as expected is stronger in the afternoon than in forenoon since rising temperature aided by increased human activities by afternoon raises the AOD. Also, we infer from table 2 that except for some of the summer and winter months, there is a positive correlation of wind speed with AOD for all other months, indicating rise of AOD with increasing wind speed. This correlation is the strongest in monsoon and autumn months possibly due to more wind speed in these months as shown by figure 2. On an annual basis, this correlation is moderately positive with a correlation coefficient of 0.46 and level of confidence above 80%. Further, this correlation is also stronger in forenoon than in afternoon during any part of measurement day. The correlation between AOD and wind direction is found negative for a

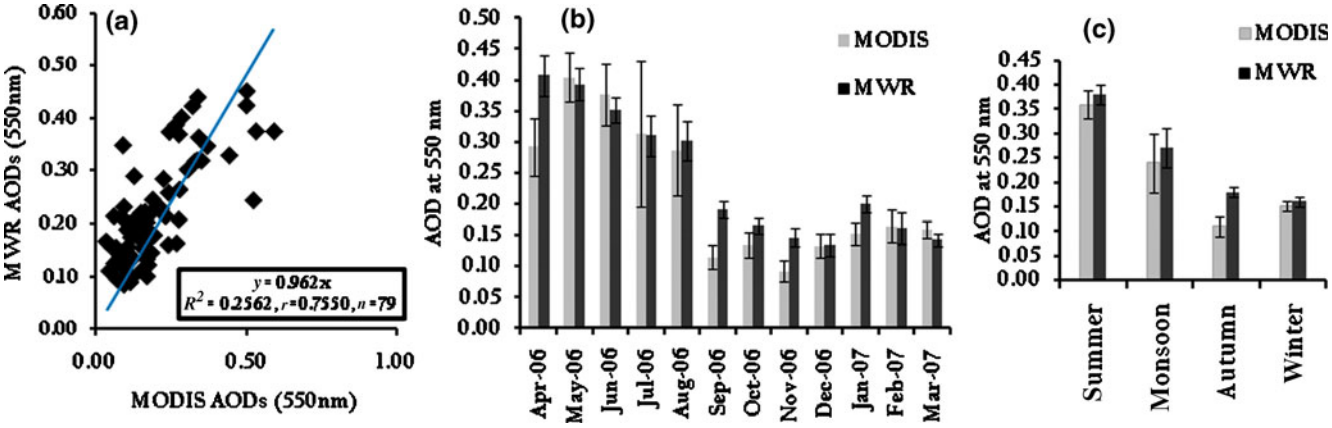


Figure 7. Comparison of MWR and MODIS: (**a**) diurnal, (**b**) monthly, and (**c**) seasonal.

majority of the months except some monsoon and winter months. It shows that AOD decreases as angle indicating direction of wind increases or veers anticlockwise and *vice versa*. In other words, as direction of wind gradually changes or shifts from south-east to south as indicated by figure 2, the AOD decreases. Thus, airmass coming from the Indo-Gangetic Plains brings more dust than the airmass coming from south-west of the present study site, i.e., from the Thar Desert. On an annual basis, this correlation is significantly negative with a correlation coefficient of −0.55 with a confidence level above 90%. This correlation is sufficiently strong in forenoon than in afternoon. Finally, we find from this table that except for the months of June, July and August, there is a positive correlation of humidity with AOD for most of the months showing rise in AOD with rising humidity. In monsoon months, reverse trend could possibly mean that there is not much rise in AOD although humidity rises sharply in these months. On an annual basis, the correlation is neither of same sign nor of significant confidence level so as to draw any conclusions.

This correlation analysis shows strong direct dependence of AOD on temperature and wind speed, while there is an inverse dependence on wind direction on monthly as well as on an annual basis. With humidity, except in monsoon months, there seems direct dependence on monthly basis but not on annual basis possibly due to correlation mismatch in monsoon months.

### 3.6 *Correlation of 'α' and 'β' with meteorological parameters*

The correlation of daily mean '$\alpha$' as well as '$\beta$' with daily mean values of meteorological parameters is not consistently of the same sign and of sufficient confidence level for different months. The '$\alpha$' *vs.* temperature correlation is found significantly negative in most of the months, while that of '$\beta$' is found positive. This trend is vindicated by annual correlation as shown in table 3 which shows a consistent negative correlation of '$\alpha$' and positive correlation of '$\beta$' with temperature at sufficiently high levels of confidence. This indicates that concentration of fine particles decreases while that of coarse particles (turbidity) increase with rising temperature and *vice versa*. This annual correlation is stronger in FN than in AN part of a day. The correlation of '$\alpha$' and '$\beta$' with wind speed has same trend as that of with temperature but it is not as strong as temperature correlation. Thus, '$\alpha$' *vs.* wind speed correlation on monthly basis is found significantly negative while that of '$\beta$' is found positive except for few months. On an annual basis, it is supported by consistent negative correlation of '$\alpha$' and positive correlation of '$\beta$' with wind speed indicating decrease in fine particle concentration and increase in turbidity when wind speed increases and *vice versa*. From '$\alpha$' and '$\beta$' *vs.* wind direction correlation analysis, we find that it is significantly positive for '$\alpha$' and negative for '$\beta$' in most of the months indicating that fine particle concentration rises and coarse particle concentration falls as wind direction shifts from east to south and *vice versa*. Thus, it can be said that fine particles are observed more if wind direction becomes more southward, i.e., from the Thar Desert of India and coarse particles are found more if wind direction is from the Indo-Gangetic Plains of India. On an annual basis, the '$\alpha$' *vs.* wind direction correlation is neither found consistently of same sign nor of sufficient confidence level, but correlation of '$\beta$' *vs.* wind direction is found negative and of significant value in FN part of a day as well as for whole day. Finally, on a monthly basis, we find that '$\alpha$' *vs.* humidity has negative correlation and '$\beta$' *vs.* humidity has positive correlation in majority of the months indicating that high humidity

Table 2. *Correlation between AODs at 500 nm and meteorological parameters.*

| Months | | Monthly correlation | | | | | | | | | | Annual correlation | | |
|---|---|---|---|---|---|---|---|---|---|---|---|---|---|---|
| | | Apr-06 | May-06 | Jun-06 | Jul-06 | Aug-06 | Sep-06 | Oct-06 | Nov-06 | Dec-06 | Jan-07 | Feb-07 | Mar-07 | FN | AN | Mean |
| Met parameters | No. of days | 2 | 5 | 7 | 3 | 4 | 11 | 3 | 6 | 7 | 13 | 5 | 13 | 12 | 12 | 12 |
| TEMP | r | 1.00 | 0.08 | 0.13 | 0.99 | 0.98 | −0.15 | 0.85 | 0.38 | 0.04 | −0.22 | −0.60 | −0.08 | 0.64 | 0.80 | 0.77 |
| | %CL | 99 | 10 | 20 | 90 | 90 | −30 | 60 | 50 | 10 | −50 | −70 | −20 | 98 | 99 | 99 |
| WS | r | 1.00 | −0.13 | −0.06 | 0.97 | 0.48 | 0.02 | 0.99 | 0.01 | −0.11 | 0.10 | −0.04 | −0.18 | 0.67 | 0.30 | 0.46 |
| | %CL | 99 | −20 | −10 | 80 | 30 | 10 | 95 | 10 | −20 | 30 | −10 | −50 | 98 | 70 | 80 |
| WD | r | −1.00 | −0.93 | 0.17 | −0.56 | 0.50 | 0.11 | −0.97 | 0.17 | 0.57 | 0.07 | 0.16 | 0.02 | −0.70 | −0.18 | −0.55 |
| | %CL | −99 | −95 | 30 | −40 | 30 | 20 | −80 | 20 | 80 | −10 | 20 | 10 | −98 | −40 | −90 |
| HD | r | 1.00 | 0.28 | −0.76 | −0.91 | −0.71 | 0.08 | −0.54 | 0.77 | 0.01 | 0.39 | 0.63 | 0.53 | 0.10 | −0.12 | 0.06 |
| | %CL | 99 | 30 | −95 | −70 | −50 | 10 | 30 | 90 | 10 | 80 | 70 | 90 | 30 | −30 | 10 |

lowers fine particle concentration while it raises coarse particle concentration possibly due to condensation of water vapour on fine aerosol particles. On an annual basis, the correlation of both '$\alpha$' as well as '$\beta$' with humidity is neither of same sign nor of sufficient confidence level in the various parts of a day.

## 4. Conclusions

The important conclusions drawn from this temporal and spectral study of AODs, Ångstrom coefficients and their dependence on meteorological parameters are as follows:

- The general trend that AODs decrease exponentially with increasing wavelength is observed with maximum value of AOD at 380 nm and at 400 nm. The high AOD at lower wavelengths indicates relatively large presence of fine particles in our atmosphere which is mainly due to anthropogenic interference in the nature.
- The AODs are high in summer, moderate in monsoon, low in winter and very low in autumn months. Annual average of AOD at 500 nm for the entire study period is found to be $0.24 \pm 0.01$ for all clear sky days.
- The fractional asymmetry factor is found negative during most of the months in this hilly region indicating that AN-AOD values are higher than FN-AODs. The negative asymmetry factor is significantly more in summer and autumn months. However, there are some monsoon and winter months when the asymmetry factor is also found to be positive.
- The AOD at 500 nm has significantly positive correlation or direct dependence on temperature and wind speed on monthly as well as on the annual basis. When correlation with wind direction is computed, it is found to be negative during most of the months as well as on the annual basis. While AOD correlation with humidity in most of the months is found to be positive, it was insignificant on annual basis.
- The value of '$\alpha$' is low in summer, medium in monsoon, high in winter and highest in autumn and early winter months, whereas '$\beta$' has opposite trend. The annual mean values of '$\alpha$' and '$\beta$' are $1.06 \pm 0.09$ and $0.14 \pm 0.01$, respectively.
- The correlation between '$\alpha$' and '$\beta$' is found to be mostly negative with few exceptions of being positive. It is found to be positive during some monsoon and winter months.
- The correlation of '$\alpha$' with temperature as well as wind speed is found to be strongly negative while that of '$\beta$' is found strongly positive in a majority of the months as well as on annual basis.

Table 3. *Correlation of monthly mean '$\alpha$' and monthly mean '$\beta$' with meteorological parameters.*

| | | '$\alpha$' | | '$\beta$' | |
|---|---|---|---|---|---|
| | | r | %CL | r | %CL |
| TEMP | FN | −0.7259 | >99 | 0.7670 | >99 |
| | AN | −0.6071 | >95 | 0.7274 | >99 |
| | Mean | −0.7673 | >99 | 0.7660 | >99 |
| WS | | | | | |
| | FN | −0.3954 | >70 | 0.6654 | >98 |
| | AN | −0.2803 | >60 | 0.2177 | >40 |
| | Mean | −0.5188 | >90 | 0.4379 | >80 |
| WD | | | | | |
| | FN | 0.2632 | >50 | −0.6702 | >98 |
| | AN | −0.1678 | >30 | 0.0242 | >5 |
| | Mean | 0.2533 | >50 | −0.4152 | >80 |
| HD | | | | | |
| | FN | −0.2338 | >50 | 0.0889 | >20 |
| | AN | 0.3070 | >60 | −0.3359 | >70 |
| | Mean | 0.1149 | >20 | 0.1284 | >30 |

With wind direction, '$\alpha$' shows positive, while '$\beta$' shows negative correlation. However, in a majority of months, with humidity, the '$\alpha$' shows negative and '$\beta$' shows positive correlation. Annually speaking, the correlation of wind direction and humidity with '$\alpha$' as well as '$\beta$' do not have strong confidence levels.

## Acknowledgements

The authors are thankful to the Director of G. B. Pant Institute of Himalayan Environment and Development, Kosi-Katarmal, Almora, Uttarakhand for providing necessary facilities at Himachal Unit of the Institute. Thanks are also due to ISRO, Bangalore for providing financial support as well as MWR through Space Physics Laboratory, Thiruvananthapuram and encouraging the inter-institutional collaborative research program. This research is supported by NASA's Giovanni, an online data visualization and analysis tool maintained by the Goddard Earth Sciences (GES) Data and Information Services Center (DISC), a part of the NASA Earth–Sun System Division.

## References

Aloysius M, Mohan M, Parameswaran K, George S K and Nair P R 2008 Aerosol transport over the Gangetic basin during ISRO–GBP land campaign-II, *Ann. Geophys.* **26** 431–440.

Ångstrom A 1961 Technique of determining turbidity of the atmosphere; *Tellus* **13** 214–223.

Ångstrom A 1964 The parameters of atmospheric turbidity; *Tellus* **16** 64–75.

Bhuyan P K, Gogoi M M and Moorthy K K 2005 Spectral and temporal characteristics of aerosol optical depth over a wet tropical location in northeast India; *Adv. Space Res.* **35** 1423–1429.

Census of India 2001 Population Totals, Director of Census Operation, part-2, Govt. of Himachal Pradesh, Shimla, India, pp. 1–79.

Charlson R J, Schwartz S E, Hales J M, Cess R D, Coakley J A, Hansen J E and Hoffman D J 1992 Climate forcing by anthropogenic aerosols; *Science* **225** 423–430.

Chiapello I, Prospero J M, Herman J and Hsu C 1999 Nimbus-7/TOMS detection of mineral aerosols over the North Atlantic Ocean and Africa; *J. Geophys. Res.* **104** 9277–9292.

Devara P C S, Pandithurai G, Raj P E and Sharma S 1996 Investigations of aerosol optical depth variations using spectroradiometer at urban station, Pune, India; *J. Aerosol. Sci.* **27** 621–632.

Devara P C S, Saha S K, Raj P E, Sonbawne S M, Dani K K, Tiwari Y K and Maheskumar R S 2005 A four-year climatology of total column tropical urban aerosol, ozone and water vapour distribution over Pune, India; *Aerosol Air Qual. Res.* **5(1)** 103–114.

Dockery D W and Rope C 1994 Acute respiratory effects of particulate air pollution; *Ann. Rev. Publ. Health* **15** 107–132.

Dumka U C, Moorthy K K, Pant P, Hegde P, Sagar R and Pandey K 2008 Physical and optical characteristics of atmospheric aerosols during ICARB at Manora Peak, Nainital: A sparsely inhabited, high-altitude location in the Himalayas; *J. Earth Syst. Sci.* **117(S1)** 399–405.

Eck T F, Holben B N, Reid J S, Dubovik O, Smirnov A, O'Neill N T, Slutsker I and Kinne S 1999 The wavelength dependence of the optical depth of biomass burning, urban and desert dust aerosols; *J. Geophys. Res.* **104** 31,333–31,350.

Gajananda K, Kuniyal J C, Momin G A, Rao P S P, Safai P D and Ali K 2005 Trend of atmospheric aerosols over northwestern Himalayan region, India; *Atmos. Environ.* **39(27)** 4817–4825.

Ganesh K E, Umesh T K and Narasimhamurthy B 2007 Unusual behavior of Angstrom turbidity parameters; *Proc. Conf. on Emerging trend on aerosols: Technology &*

*application (IASTA 2007)*, New Delhi, India, November 14–16, **18(1&2)** 91–92.

Ganesh K E, Umesh T K and Narasimhamurthy B 2008 Site specific aerosol optical thickness characteristics over Mysore; *Aerosol Air Qual. Res.* **8(3)** 295–307.

Ganguly D, Jayaraman A and Gadhavi H 2006 Physical and optical properties of aerosols over an urban location in western India: Seasonal variabilities; *J. Geophys. Res.* **111** D24206.

Gautam R, Hsu N C, Lau K M and Kafatos M 2009 Aerosol and rainfall variability over the Indian monsoon region: Distributions, trends and coupling; *Ann. Geophys.* **27** 3691–3703.

Gogoi M M, Bhuyan P K and Moorthy K K 2008 Estimation of the effect of long-range transport on seasonal variation of aerosols over north eastern India; *Ann. Geophys.* **26** 1365–1377.

Goyal J K and Sharma J N 1963 *Mathematical statistics* (Meerut, India: Krishna Prakashan Mandir), pp. 378–476.

Holben B N, Tanr D, Smirnov A, Eck T F and 19 coauthors 2001 An emerging ground-based aerosol climatology: Aerosol optical depth from AERONET; *J. Geophys. Res. Atmos.* **106** 12,067–12,097.

Iqbal M 1983 *An introduction to solar radiation* (Toronto: Academic Press), pp. 1–118.

Jaenicke R and Schutz L 1978 Comprehensive study of physical and chemical properties of the surface aerosol in the Cape Verde Islands region; *J. Geophys. Res.* **83** 3585–3599.

Jayaraman A 2001 Aerosol radiation cloud interaction over tropical Indian Ocean prior to onset of the summer monsoon; *Curr. Sci.* **81(11)** 1437–1445.

Kaskaoutis D G, Kambezidis H D, Hatzianastassiou N, Kosmopoulos P G and Badarinath K V S 2007 Aerosol climatology: Dependence of the Angstrom exponent on wavelength over four AERONET sites; *Atmos. Chem. Phys. Discuss.* **7** 7347–7397.

Kaufman Y J and Fraser R S 1997 The effect of smoke particles on clouds and climate forcing; *Science* **277** 1636–1639.

Kaufman Y J, Tanre D, Remer L A, Vermote E F, Chu A and Holben B N 1997 Operational remote sensing of tropospheric aerosol over land from EOS moderate resolution imaging spectro-radiometer; *J. Geophys. Res.* **102(D14)** 17,051–17,067.

Kaufman Y J, Ichoku C, Giglio L, Korontzi S, Chu D A, Hao W M, Li R R and Justice C O 2003 Fire and smoke observed from the Earth Observing System MODIS instrument: Products, validation, and operational use; *Int. J. Remote. Sens.* **24(8)** 1765–1781.

Kumar S, Manoj M J, Dewara P C S, Pandithurai G and Safai P D 2007 Aerosol characteristics variations in different environments over Indian Region; *Proc. Conf. on Emerging trend on aerosols: Technology & application (IASTA 2007)*, New Delhi, India, 14–16 November, **18(1&2)** 293–297.

Kuniyal J C, Vishvakarma S C R, Badola H K and Jain A P 2004 *Tourism in Kullu valley: An environmental assessment* (eds) Bishen Singh and Mohindra Pal Singh, Dehradun, India, pp. 1–210.

Kuniyal J C, Thakur Alpana, Tripathi Smita, Thakur H K, Sharma S, Oinam S S, Pant P, Hegde P and Dumka U C 2006 Aerosols characteristics at high altitude locations of Kullu–Manali in the northwestern Himalaya during ICARB; In: *Proc. First Post-Campaign meeting of ICARB & Meeting of the WG-II of ISRO–GBP, Geosphere Biosphere Programme (I-GBP)*, Space Physics Laboratory, VSSC, Thiruvananthapuram, 25–27 October, pp. 1–232.

Kuniyal J C, Rao P S P, Momin G A, Safai P D and Ali K 2007 Trace gases behavior in sensitive area of Northwest Himalaya – A case of Kullu Manali tourist complex, India; *Ind. J. Radio Space Phys.* **36** 197–203.

Kuniyal J C, Thakur A, Thakur H K, Sharma S, Pant P, Rawat P S, and Moorthy K K 2009 Aerosol optical depths at Mohal-Kullu in the northwestern Indian Himalayan high altitude station during ICARB; *J. Earth Syst. Sci.* **118(1)** 41–48.

Kunzli N, Kaiser R, Medina S and Studnicka M 2000 Public-health impact of outdoor and traffic-related air pollution: A European assessment; *Lancet* **356** 795–801.

Levy R C, Remer L A and Dubovik O 2007 Global aerosol optical properties and application to moderate resolution imaging spectroradiometer aerosol retrieval over land; *J. Geophys. Res.* **112** D13210.

Maheskumar R S, Devara P C S, Ernest R P, Dani K K, Saha S K and Sonbawne S M 2000 Study of atmospheric turbidity parameters using multichannel solar radiometer at Pune (India); *Ind. Aerosol Sci. Tech. Assoc. Bull.* **13(1)** 193–196.

McCartney E J 1976 *Optics of the atmosphere* (New York: John Wiley), pp. 216–228.

Misra A, Jayaraman A and Ganguly D 2008 Validation of MODIS derived aerosol optical depth over Western India; *J. Geophys. Res.* **113** D04203.

Moorthy K K, Nair P R and Murthy B V K 1991 Size distribution of coastal aerosols: Effects of local sources and sinks; *J. Appl. Meteor.* **30** 844–852.

Moorthy K K, Niranjan K, Narsimhamurty B, Agashe V V and Murthy B V K 1994 *Characteristics of aerosol spectral optical depths over India*; ISRO–IMAP-Scientific Report: SR-43–94, pp. 1–78.

Moorthy K K, Satheesh S K and Krishna Murthy B V 1997 Investigations of marine aerosols over the tropical Indian Ocean; *J. Geophys. Res.* **102** 18,827–18,842.

Moorthy K K, Satheesh S K and Murthy B V K 1998 Characteristics of spectral optical depths and size distributions of aerosols over tropical regions; *J. Atmos. Solar Terr. Phys.* **60** 981–992.

Moorthy K K, Niranjan K, Narsimhamurty B, Agashe V V and Murthy B V K 1999 *Aerosol climatology over India: ISRO–GBP*; MWR network and database, Scientific Report: SR-03–99, pp. 1–30.

Moorthy K K and Pillai P S 2004 *Aerosol climatology and effects-II: Characteristics of near surface aerosols at Thumba*; ISRO–GBP: SR 06, pp. 1–83.

Moorthy K K, Babu S S and Satheesh S K 2007 Temporal heterogeneity in aerosol characteristics and the resulting radiative impact at a tropical coastal station – II: Direct short wave radiative forcing; *Ann. Geophys.* **25** 2308–2320.

Moorthy K K, Satheesh S K, Babu S S and Dutt C B S 2008 Integrated campaign for aerosols, gases and radiation budget (ICARB): An Overview; *J. Earth. Syst. Sci.* **117** 243–262.

Oberdorster G, Ferin J, Penney D P, Soderholm S C, Gelein R and Piper H C 1990 Increased pulmonary toxicity of ultrafine particles to lung lavage studies; *J. Aerosol Sci.* **17** 361–364.

Parameswaran K, Nair P R, Rajan R and Ramana M V 1999 Aerosol loading in coastal and marine environments in the Indian Ocean region during winter season; *Curr. Sci.* **76** 947–955.

Pant P, Hegde P, Dumka U C, Saha A, Srivastava M K and Sagar R 2006 Aerosol characteristics at a high-altitude location during ISRO–GBP Land Campaign-II; *Curr. Sci.* **91** 1053–1061.

Prasad A K and Singh R P 2007 Comparison of MISR–MODIS aerosol optical depth over the Indo-Gangetic basin during the winter and summer seasons (2000–2005); *Remote Sens. Environ.* **107** 109–119.

Penndorf R 1957 Tables of the refractive index for standard air and the Rayleigh scattering coefficient for the spectral region between 0.2 and 20.0 μ and their application to atmospheric optics; *J. Opt. Soc. Am.* **47** 176–182.

Ramanathan V, Crutzen P J, Kiehl J T and Rosenfeld D 2001 Aerosol, climate and the hydrological cycle; *Science* **294** 2119–2124.

Ramanathan V, Ramana M V, Podgorny I A, Pradhan B B and Shrestha A B 2003 The direct observation of large aerosol radiative forcing in Himalayan region; *J. Geophys. Res. Lett.* **31** L05111, doi: 10.1029/2003GL018824.

Remer L, Kaufman Y J, Tanre D, Mattoo S, Chu D A, Martins J, Li R-R, Ichoku C, Levy R C, Kleidman R G, Eck T F, Vermote E and Holben B N 2005 The MODIS aerosol algorithm, products and validation; *J. Atmos. Sci.* **62(4)** 947–973.

Russell P B, Livingston J M, Dutton E G, Pueschel V, Reagon J A, Defoor T E, Box M A, Allen D, Pilewskie P, Herman B M, Kinnie S A and Hofmann D J 1993 Pinatubo and pre-pinatubo optical depth spectra: Mauna Loa measurements, comparisons, inferred particle size distribution, radiative effects and relationship to Lidar data; *J. Geophys. Res.* **98** 22,969–22,985.

Russell L M, Pandis S N and Seinfeld J H 1994 Aerosol production and growth in marine boundary layer; *J. Geophys. Res.* **99** 20,989–21,003.

Satheesh S K, Moorthy K K and Srinivasan J 2004 *Introduction to aerosols and impacts on atmosphere: Basic concepts*; ISRO–GBP Scientific Report: SR 05, pp. 1–36.

Satheesh S K, Deepshikha S and Srinivasan J 2006 Impact of dust aerosols on Earth–atmosphere clear-sky albedo and its short wave radiative forcing over African and Arabian regions; *Inter. J. Remote Sens.* **27** 1691–1706.

Schuster G L, Dubovik O and Holben B N 2006 Ångström exponent and bimodal aerosol size distributions; *J. Geophys. Res.* **111** D07207.

Seinfeld J H and Pandis S N 1998 *Atmospheric chemistry and physics: From air pollution to climate change* (New York: John Wiley and Sons Inc), pp. 292–293.

Sharma N L, Kuniyal J C, Singh M, Negi A K, Singh K and Sharma P 2009 Number concentration characteristics of ultrafine aerosols (atmospheric nanoparticles/aitken nuclei) during 2008 over western Himalayan region Kullu–Manali, India; *Ind. J. Radio Space Phys.* **38** 326–337.

Sharma A R, Kharol S K, Badarinath K V S and Singh D 2010 Impact of agriculture crop residue burning on atmospheric aerosol loading – a study over Punjab State, India; *Ann. Geophys.* **28** 367–379.

Shaw G E, Regan J A and Herman B M 1973 Investigation of atmospheric extinction using direct solar radiation measurements made with multiple wavelength radiometers; *J. Appl. Meteorol.* **12** 374–380.

Shaw G E 1976 Error analysis of multi-wavelength sun photometry; *Pure Appl. Geophys.* **114** 1–14.

Shaw G E 1982 Solar spectral irradiance and atmospheric transmission at Mauna Loa Observatory; *Appl. Opt.* **21** 2006–2011.

Subbaraya B H, Jayaraman A, Moorthy K K and Mohan M 2000 Atmospheric aerosol studies under ISRO–GBP; *J. Ind. Geophys. Union* **4** 77–90.

Tegen I, Lacis A and Fung I 1996 The influence of mineral aerosol from distribution soils on the global radiation budget; *Nature* **380** 419–422.

Tomasi C, Prodi F, Sentimenti M and Cesari G 1983 Multiwavelength sun photometers for accurate measurements of atmospheric extinction in the visible and near-IR spectral range; *Appl. Opt.* **22** 622–630.

Tripathi S N, Dey S, Chandel A, Srivastava S, Singh R P and Holben B N 2005 Comparison of MODIS and AERONET derived aerosol optical depth over the Ganga Basin, India; *Ann. Geophys.* **23** 1093–1101.

Verma N, Bagare S P, Ningombam S K S and Singh R B 2010 Aerosol optical properties retrieved using Skyradiometer at Hanle in western Himalayas; *J. Atmos. Solar Terr. Phys.* **72** 115–124.

Wang Y, Xin J, Li Z, Wang S, Wang P, Hao W M, Nordgren B L, Chen H, Wang L and Sun Y 2008 Seasonal variations in aerosol optical properties over China; *Atmos. Chem. Phys. Discuss.* **8** 8431–8453.

Xin J, Wang Y, Li Z, Wang P, Hao W-H, Nordgren B L, Wang S, Liu G, Wang L, Wen T, Sun Y and Ho B 2007 Aerosol optical depth (AOD) and Ångström exponent of aerosols observed by the Chinese Sun Hazemeter Network from August 2004 to September 2005; *J. Geophys. Res.* **112** D05203, doi: 10.1029/2006JD007075.

*MS received 19 January 2011; revised 5 September 2011; accepted 8 September 2011*